6333

FTD-TT- 63-81

402591

TRANSLATION

HEAT POWER ENGINEERING
(SELECTED ARTICLES)

FOREIGN TECHNOLOGY DIVISION

AIR FORCE SYSTEMS COMMAND

WRIGHT-PATTERSON AIR FORCE BASE

OHIO

UNEDITED ROUGH DRAFT TRANSLATION

HEAT POWER ENGINEERING (SELECTED ARTICLES)

English Pages: 21

SOURCE: Russian Periodical, Teploenergetika, Nr 8, 1962, pp 47-51, 51-55

S/96-62-0-8

THIS TRANSLATION IS A RENDITION OF THE ORIGINAL FOREIGN TEXT WITHOUT ANY ANALYTICAL OR EDITORIAL COMMENT. STATEMENTS OR THEORIES ADVOCATED OR IMPLIED ARE THOSE OF THE SOURCE AND DO NOT NECESSARILY REFLECT THE POSITION OR OPINION OF THE FOREIGN TECHNOLOGY DIVISION.	PREPARED BY: TRANSLATION SERVICES BRANCH FOREIGN TECHNOLOGY DIVISION WP-AFB, OHIO.

TABLE OF CONTENTS

Calculating Radial Overflows in a Turbine Stage

by

G.V.Zhukovskiy

Presented are experimental data on the testing of gas turbine stages with cylindrical boundaries of flow-through part and D/l = 4,8. A comparison was made with the testing calculations using simplified and inverse equations of radial equilibrium. It was shown, that the divergences between experimental and calculated data are due to final phenomena and the flow through.

Among problems, connected with raising the efficiency of the flow through part of modern turbines , the problem of increasing the effectiveness of stages with small D/l occupies one of the focal points. It was established that the use of a generally adopted in industrial practice calculation method, based on the integration of a simplified equation of rational equilibrium, for the calculation of turbine stages with small D/l leads to substantial errors. The effort to increase the efficiency of the latter stages leads to the necessity of doing away with the use of simplified formulas and requires the creation of a more perfect calculation model. It is understood, that to agreefor such a change in basic formulas, which leads to an increase in volume of calculation operations, is advisable only for these stages, for which this complication will allow to raise the efficiency by any noticeable value. In this way, the path of developing methods for the calculation of flow dimensionality should be not only the formulation of necessary calculation formulas, but also the indication of boundaries, in which the use of given formulas appears to be suitable. However in one of the published reports this aspect of the problem has not been sufficiently elucidated. Furthermore, an impression can be gained from examining the individual reports,

that their authors do recommend the abandonment of using the simplified equation of radial equilibrium when calculating stages with relatively large D/l. And so, in report by Ya.A.Sirotkin [L.1] in the role of an example of using the method developed by the author is given a check calculation of stages with cylindrical boundaries of the flow through part and $D_{aver}/l = 6$. Although it is pointed out in the report, that the use of the proposed method is recommended first of all for stages with sharply expanding flow through section and D/l = 2-4, the author emphasizes, that the calculation of stages, having cylindrical outlines of the flow through part and $D_{aver}/l=6$ should be made not only from gap to gap, but also in the zone, occupied by rims, with consideration of constraining and radial velocity components.

To experimentally confirm the latter statement it was found possible to expand in necessary direction the investigation involving the creation of a family of gas turbine stages, carried out at the TSKTI upon the initiative of A.M.Zavadskiy. In the role of investigation object was used a stage with cylindrical outline of flow through part ($D_{aver}/l=4.86$). Detailed experimental data, obtained on this stage were compared with reasults of check calculations by the simplified as well as by the inverted equations of radial equilibrium.

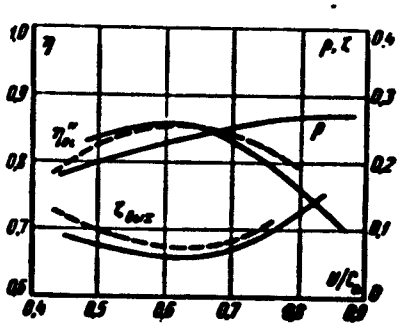

Fig.1.Stage Characteristics η''_{in} -internal efficiency without use of output velocity; η'_{ol}-internal efficiency at full utilization of output velocity; ζ_{outp}-loss from output velocity on central diamet; ρ-mean reaction. Solid lines-experiment, dotted-calculation.

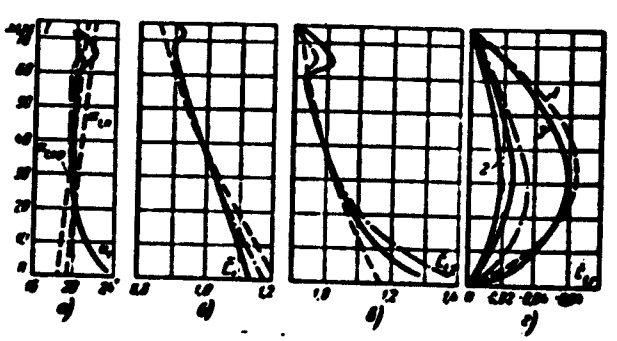

Fig.2.Flow parameters behind guiding apparatus at $\lambda_0 = 0.543$ $a-a_{cr}$ α -angles of flow output in stages by flow data of flat grids; a_{cr} -effective angle of grid; b-$c_1 = c_1/c_{1aver}$-relative isocentropic velocity

Fig.2,continued

c- $\bar{c}_{1z} = c_{1z}/c_{1z\ aver}$ -relative axial projection of velocity c_1; d- $\bar{c}_{1r} = c_{1r}/c_{1z\ aver}$-relative radial projection of velocity c_1; 1-calculated by equation (1); 2-experiment at $\lambda_0 = 0.62$; 3-calculated by equation (3) Solid line-stage; dash-dot- annular grid; plotted-calculation.

Before analyzing the obtained results, it is necessary to briefly discuss the method of planning the tested stage and the method of processing the experimental material.

The guiding apparatus of the stage has cylindrical vanes with TS2A-40 profile. The output edges of the vanes were directed radially. On the central diameter the grid pitch/chord profile ratio was 0.717 and the effective angle (arcsin ration of neck to pitch) was $\alpha_{1\ ef} = 19°40'$. During the calculation the angles of flow outcome from the guiding apparatus were considered as fixed (given), whereby their numerical values were accepted in accordance with flow through data of flat grids. On the central diameter of the working wheel were given relative pitch of vanes 0.75 and effective angle $\beta_{2\ eff} = 25°20'$. In this way, the planning of stages was brought down to calculating the twist of working vanes. It was assumed thereat, that the parameters of flow at the input into the stage and the static pressure behind the working wheel - constant values with respect to height and pitch. The calculated condition of stages was characterized by the given velocity $\lambda_0 = c_0/\alpha_0^* = 0.676$ (where $\alpha_0^* = \sqrt{kgRT_0^*}$ - speed of sound over decelerated parameters at input) and by the ratio $u/c_0 = 0.596$.

Stage is calculated on the basis of a simplified equation of radial equilibrium

$$\frac{dp}{dr} = \frac{1}{vg} \cdot \frac{c_u^2}{r}. \qquad (1)$$

The angles of flow outcome from the guide apparatus are known, consequently, by integrating (1) it is possible to obtain a velocity distribution along the height of the inter-rim gap:

$$\bar{c}_1 = c_1/c_{1\ cp} = \exp\left(-\int_{\bar{r}}^{\bar{r}} \frac{\cos^2\alpha_1}{r}\, dr\right), \qquad (2)$$

where $c_{1\ aver}$-velocity on central diameter; $\bar{r} = r/r_{aver}$ - given function.

It is apparent, that to satisfy simultaneously equation (1) and condition $p_2 = const$, it is necessary to have an axial outcome of the flow from the stage ($c_2 = c_{2z}$).

The twist of the output edge of the working vane was made so, that at any given radius in the sections in front and in the rear of the working wheel the current density remained constant: $c_{1a}/v_1 = c_2/v_2$.

Mathematical processing of section profiles of the working vane was done by the method introduced by A.L.Sherstyuk [L.2].

Examinations of stages were made at constant initial air parameters and constant counter pressure, which corresponded with the conditions of calculation. When analyzing the experimant the efficiency of the stage is determined by an ordinary method, adopted at the TSKTI, whereby the loss due to leakage through the radial gap above the working vanes was calculated by formula introduced by A.M.Zavadovskiy [L-3]. The radial gap over the working vanes was 1.5 mm, which at a 75 mm vane height and mean diameter of 365 mm corresponded to 2% of height and 2,4% of frontal area of the vane. The maximum efficiency without the use of output velocity reached $\eta''_{oi} = 0.86$, and at total utilization of output velocity $\eta'_{oi} = 0.92$.

In fig.1 are given dependence graphs η'_{oi}, η''_{oi}, $zeta_{outp}$ and φ upon u/c_o. Solid lines indicate magnitudes of these values, calculated on the basis of experimental data and the dotted lines -calculated values. At such a value φ was calculated asa mean arithmetic value between root and peripheral reaction, i.e. $\varphi = 0.5\,(\varphi_p + \varphi_k)$ and the loss with output velocity on the mean diameter zeta = $(c_2/c_o)^2$.

A detailed investigation of the flow in the gap and behind the stage was made at two conditions. Results of analyzing the condition,close to calculated and characterized by given velocity $\lambda_o = 0.543$, ratio $u/c_o = 0.615$ and Re_1 number = $5.5 \cdot 10^5$, are shown in fig.2-5 by solid lines.

The velocities and their projections are refered to magnitudes of corresponding values on thecentral diameter of thevery same section. The rates of the flow beyond the guide apparatus (fig.2,b and c) were calculated by isocentropic fluctuations, and on the working wheel (fig.3,a and c) and behind the stage (fig.4b, and c) - with consideration of losses. Radial velocities are given in fractions of axial velocity on

mean diameter of corresponding section. And so, on fig.2,d is shown the relative radial velocity behind the guide apparatus:

$$\bar{c}_{1r} = c_{1r}/c_{1}, \; c_{1r} = \bar{c}_{1r} \sin \gamma_1. \quad (4)$$

where gamm$_1$-angle betwen meridional and axial velocities which during the analysis of the experiment is calculated as a ratio

$$\gamma_1 = \operatorname{arc\,tg} \frac{\Sigma \Delta l_1 - \Sigma \Delta l_0}{\Delta z_1}. \quad (5)$$

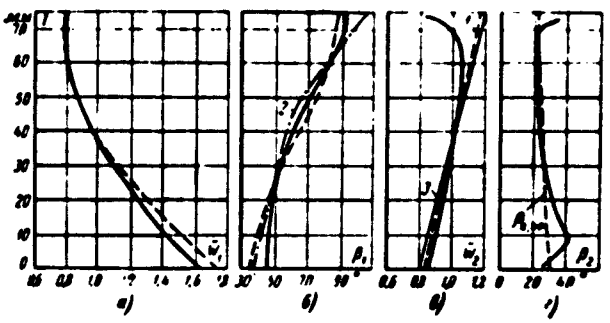

Fig.3,Flow parameters in relative movement at $\lambda_0 = 0.543$; $u/c_0 = 0.615$
a - $\bar{w}_1 = w_1/w_1$ aver-relative velocity at input into working wheel; b - β_1 - angle at input into workingwheel ; 2-mean angle of profile; c-$\bar{w}_2 = w_2/w_2$ aver-relative velocity at output from working wheel ; 1-calculation by equation (1); 3-calculation by equation (3); d- $\frac{1}{2}$-angle of flow at output from working wheel.

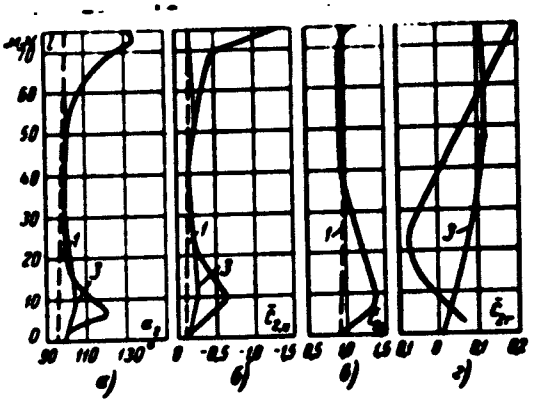

Fig.4,Flow parameters behind working wheel at $\lambda_0 = 0.543$; $u/c_0 = 0.615$
a-α_2 - angle of flow output; b- $\bar{c}_{2t} = c_{2t}/c_{2z}$,aver - relative circumferential projection of velocity c_2; c- $c_{2z} = c_{2z}/c_{2z}$, aver- relative axial projection ov velocity c; d- c_{2r} - relative radial projection of velocity. 1-calculated by equation (1); 3-calculated by equation (3)

where Δz_1 - axial width of guide apparatus; Δl_1 and Δl_0 - sectional height of flow through section in front and behind the guide apparatus, through which identical amounts of flow pass.

The relative radial velocity behind the working wheel $\bar{c}_{2r}$ (fig.4,d) was calculated in an analogous manner.

The loss coefficient in the guide apparatus zeta$_n$ (fig.5,e) is determined by formula

$$\zeta_n = 1 - \left(\frac{\lambda_{1\Phi}}{\lambda_1}\right)^2. \quad (6)$$

where $\lambda_{1F} = f(\bar{p}^*_1)$ - fictitious velocity corresponding to relative total pressure in inter-rim gap.

When processing experimental data the loss coefficient on the working wheel zeta $_{w.w}$. (fig.5,d) is determined as follows:

$$\zeta_{w.w} = 1/(1-\rho)\zeta_{a} - \zeta_{out} - \eta_{w}. \quad (1)$$

In this formula the rho values of the reactivity degree (fig.5,a) of the coefficient $\eta_{o} = 2\lambda_{u}/\lambda_{a}^{2}$ ($\lambda_{1}\cos\alpha_{1} - \lambda_{2}\cos\alpha_{2}$) fig.5,b) and values of energy loss coefficients zeta$_{outp}$ and zeta$_{n}$ (fig.5,c and e) - values, found on the corresponding radius in accordance with experimental data.

In addition to the basic test program, measurements were also made on the guide apparatus with working wheel removed. The chamber, forming in place of the removed wheel, was covered with a special ring. On the mean diameter behind the annular grid is established the pressure drop, equal to the drop on the mean diameter at the guide apparatus when testing the stages. Results of these measurements are given in fig.2,a b and c and d by dash-dot lines. It is evident from the drawings that the mentioned differential equality on the mean diameter is insufficient to assure identical parameters over the entire height of the inter-rim gap. This indicates, that the performance of the annular grid guide without turbine wheel is not always equivalent to performance of the guide apparatus in stage conditions. It is apparent, that to use the results of blowing through the annular guide of the grid directly in the calculation of stages, it is necessary behind the annular grid to assure such pressure distribution, which would correspond to reaction distribution along the height of stages.

In addition to experimental data in fig/2-5 are plotted values, which were obtained through calculation. Two spot calculations were made. The first one was made on the basis of a simplified equation of radial equilibrium (1), whereby the condition of the work was fixed by experimentally established parameters of deceleration at the input into the stage p_0^*, T_0^*, given velocity on the mean diameter in the inter-rim gap λ_1 aver = f ($\bar{p}_1$ aver) and ratio u/c_0. It is evident, that the use of equation (1) in the given case has no strict mathematical foundation. The fact is, equation (1) is valid for

cylindrical flow. The angles of flow out put from the guide apparatus, on the basis of which by formula (2) was calculated the velocity distribution in inter-rim space, are due to the geometry of the guide apparatus selected by us and, as shown by calculation and experiment (fig.2,d) they did not provide flow cylindricity in the inter-rim gap. The use of equation (1) is ordinarily argumented by the fact, that the magnitude of radial velocity is low. But equation of radial equilibrium includes not only the radial velocity, but its derivative, which in known instances may appear to be compatible with c_u^2/r. For the given stage the maximum calculated value dc_r/dt in inter-rim gap reached 7% of c_u^2/r.

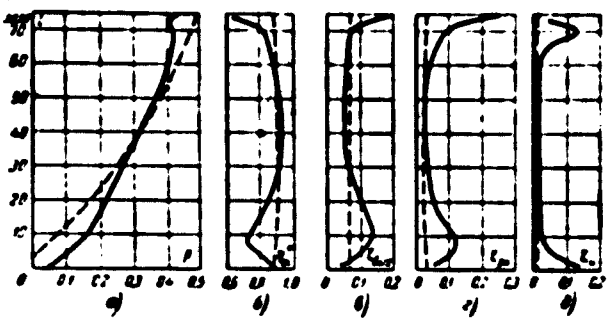

Fig.5. Reaction, efficiency and losses in stage at $\lambda_0 = 0.543$; $u/c_0 = 0.615$ a-rho-reaction; b-η''_{oi}-internal relative efficiency without use of output velocity; c- $zeta_{outp} = (c_2/c_0)^2$-loss with output velocity; d-$zeta_{w.w.}$-loss on working wheel; e- $zeta_n$-loss in guide apparatus. dotted line-calculated values.

The second calculation was made on infinitely thin vanes with consideration of radial velocity components in gap and behind the stage. The calculation method was developed at the TSKTI by M.I.Zhukovskiy and A.P.Tarabrin. The working condition of the stage was given in accordance with experimentally determined deceleration parameters at the input into the stage p_0^*. T_0^*, parameters of air delivery G and the rpm n.

$$\frac{dp}{dr} = \frac{1}{vg}\left(\frac{c_u^2}{r} - \frac{dc_r}{dt}\right) = \frac{1}{vg}\left(\frac{c_u^2}{r} - c_r\frac{\partial c_r}{\partial r} - c_r\frac{\partial c_r}{\partial z}\right) \quad (3)$$

The calculation was made by the method of subsequent approximations. In the first approximation the current surfaces were made cylindrical, and the distribution of velocities in the gap was adopted by equation (2). The axial velocity on the mean diameter behind the guide apparatus, which in given case played the role of an integration constant, was taken from experimental results. Leakage through the radial gap

above the working vanes was calculated by the A.M.Zavadovskiy formula, and the peripheral current line was made with consideration of overlapping. An agreement ina number of solutions has been attained after calculating three approximations. For the inter-rim gap the velocities of third approximation in relative values at a scale fig.2,b and c, have practically coincided with the calculations according to equations (1) and (2). On the other hand, it is evident on fig.2, that the difference between calculated and experimental values on the end sections, reached noticeable values. On the center part of the vane were measured the magnitudes of angles (fig.2,a) and losses (fig.5,d) which coincided with values obtained for flat grids of corresponding pitch. The slope of curves of angles and total pressures along the peripheral section is due to secondary final flows. A similar picture is usually found when directing the flow against flat as well as annular grids. The flow characteristics near the root diameter are also due to secondary, final phenomena, but, as is evident from fig.2,a, the nature of the root secondary flow is different from the one which takes place on the periphery.

The mentioned chart of angle and loss distribution along the height of inter-rim gap appears to be typical for turbine stages. The fact is, analogous experimental data have been obtained by many authors, particularly V.G.Tyryshkin [L-4] and Kh.L. Babenko [L.5].

Structural characteristics of a flow, passing through an annular guide grid, have been investigated by many researchers. It is shown in the calculation by M.Ye.Levina and P.A.Romanenko [L.6] that behind the annular grid, the geometry of which is close to the one adopted in our investigation, the radial overflows should be directed toward the root, have a maximum near the mean diameter and in the zone of subsonic velocities decrease with the rise in M-number. These mathematical deliberations have been fully confirmed during the experiment (fig.2,d), in spite of the fact that in the given case the radial velocities were small (not more than 4% of axial velocity on the mean diameter).

In fig.3 and 4 are shown the flow parameters in relative movement in the working wheel and in absolute movement behind the stage. On the drawings are presented values which are usually in operation when calculating flow through part, and that is why the graphs require bo special explanations. In view of the limited volume of the given report it is difficult to give here a description of the calculation order of the values listed in fig.3 and 4,nct to give a detailed analysis of individual graphs. It must be underlined that, as is evident from fig.3 and 4, the difference between calculation by simplified (1) and inverted (3) equations is small in comparison with the divergences between calculated and experimental values on the root and peripheral sections of the working vane. It can be said, that these dive gences on the working wheel are relatively larger, than on corresponding radii of root and peripheral sections of interrim gapIn addition to the above mentioned final (terminal) flows, the cause of the mentioned divergences appears to be the fact that the distribution of parameters on the working wheel and behind stage produces a considerable effect of the flow through through the radial gap and a clogging of the passing section on account of bodies of working vanes. Calculation of the narrowing [L-1] shows, that in comparison with curve 3 in fig.4,d, on the root section will take place additional current line deviations in direction toward the bushing, and on the peripheral section - toward the body of the turbine.

Comparisons showed,that both calculations - the first one by the simplified (1) and the second by the developed (3) equation of radial equilibrium give close results i.e.in the case under consideration calculation of additional members in equation of radial equilibrium has not helped to eliminate divergences between distribution in height of calculated and experimental flow parameters. This is due to the fact that, first of all, radial velocities in tested stage are not too high and, on the other hand, both calculations were based on one and the same initial data on the distribution of output angles and losses along the height of the grids.

It is concluded on the basis of above made statements that for the given stage the deficiencies of ordinary calculation schemes lie not only in the incompleteness of equation (1) as compared with equation (3), but in a much higher degree in the absence of a proper calculation of the effect of secondary end flows, and of the flow through through the radial gap over the working vanes.

Many investigations have been devoted to the analysis of mentioned phenomena, e.g. [L.7 and 8] but a sufficiently perfect reply, suitable for plant calculations has not been obtained until now. Putting aside the question on whether the practical calculations should include secondary flows for stages with quite lengthy vanes, it can be said, that for stages, similar to the one examined in this investigation (i.e. with cylindrical boundaries of flow through section and $D_{aver}/l = 4,8$), the complication of the spatial flow calculation is not justified. It is understood, that the conclusion made does in way reduce the actuality of further developing the method of calculating spatial flow in a turbine stage with lower D/l and noncylindrical outlines of the flow through section. Further research has to be organized so that to determine the boundary it is advisable to use these or other calculation schemes for turbine stages.

Conclusions

Testing of stages, planned on the basis of a simplified equation of radial equilibrium, have shown fine conformity between experimental and calculated relative parameters. The difference between experiment and calculation reaches a noticeable magnitude along end sections and is due to secondary, end flows, and on the working wheel, in addition, to the flow-through through the radial gap over the working vanes.

For stages, the geometry of which is closed to the geometry of the investigated stage, it is inadvisable to complicate the calculation by solving the developed equation of radial equilibrium.

Distribution in height of flow through section of flow parameters when working wheel is removed differs from the distribution obtained in inter-rim gap when testing stages.

Literature

1. Ya.A.Sirotkin; Izvestiya Akademii Nauk SSSR.Mechanics and Machine Construction, 2,1961

2. A.N.Sherstyuk, Teploenergetika, No.8, 1955

3. A.A.Zavadovskiy. Bases of Planning the Flow-Through Part of Steam and Gas Turbines, Mashgiz, 1960

4. V.G.Tyryshkin, Izvestiya Akademii Nauk SSSR,Otdel.Tekhn.Nauk, No.6, 1954

5. Kh.L.Babenko ; Teploenergetika No.2, 1961

6. M.Ye.Levina; P.A.Romanenko, Transactions of the KhPI,vol 29, ed.2, 1960

7. V.S.Beknev; Teploenergetika No.1, 1961

8. N.M.Ukhkov; Calculating Aerodynamic Characteristics of a Vane Apparatus,Mashgiz 1955.

Measuring Pressure Pulsations and Dynamic Stresses on Rotating Vanes of an Axial Compressor

by

G.S.Samoylovich
I.M.Fis'man

Described are studies of pressure pulsations and the dynamic stresses of axial compressor vanes caused by them. The investigations were conducted by the tensometric sounding method. The condition at which the phenomenon of rotating flow separation takes place, was investigated.

The phenomenon of rotating separation, which originates in stages of an axial compressor at a reduction of gas consumption to below a certain minimum point, is well known at present time. There is a considerable number of experimental reports, in which the general laws of this phenomenon are described. The Moscow Energetics Institute conducted investigations on special single-and multi-stage compressor models, and on natural machines, which have been examined on the LMZ stand and on an operating gas turbine installation of the Shatsk electric power station. A part of these investigations was conducted in cooperation with the LMZ [L.1-3] .

In the given report are described new investigations, devoted to measuring pressure pulsations and dynamic stresses caused by them.

The investigations were carried out on a two-stage axial compressor with vaning K-4, used in compressor GTU-12 LMZ.

The geometrical parameters of the flow through part of this compressor are given in table 1.

In addition to the conventional measuring apparatus with which the compressor is equipped for the purpose of determining characteristics, were also applied low-

inertia measuring devices, used for studying nonstationary phenomena.

Name of values	Guide appar	Working wheel	Guide appar	Working wheel	Rectifying apparatus
Outer diameter d_{outer} mm...	360	360	360	360	360
Bush ratio d_{inter}/d_{out}...	0.61	0.617	0.625	0.637	0.654
Height of vanes l, mm	70	69	67	65	64
Chord of vanes ($d=d_{aver}$) b, mm...	22.5	30	22.5	30	22.5
Relative height of vanes l/b...	3.11	2.3	2.98	2.2	2.84
Number of vanes z...	60	35	60	35	60
Pitch of vanes ($d=d_{aver}$)t, mm...	19	25.3	15.1	28	17
Relative pitch t/b...	0.845	0.846	0.67	0.765	0.756
Angle of vane setting ($d=d_{aver}$) β_y...	79°	57° 40'	85°	37° 40'	86°
Radial gap δ, mm...		0.3		0.3	
Relative radial gap δ/l...		0.23		0.22	

To measure pulsations of total pressure and static pressure low-inertia tensometric probes, developed at the LKI =Moscow Energetics Inst, we used.

A description of the construction of these probes and their investigations is given in [L.3]. In this report, in contrast to [L.3] were used probes with equilibrating chamber (fig.1), which appear to be universal and can be used in a flow with low, as well as high static pressure. The receiving chamber of such a probe has minimum dimensions. On the other side the membrane is made a capacious chamber, into which air can penetrate through the choke tube (throttle tube). The volume of the chamber and the resistance of the throttle tube are figured in such a way, that when measuring the pulsating pressure the variable pressure component behind the membrane constitutes only several percentages of the variable component in front of the membrane. Constant pressure components are equilibrated, and that is why the membrane can be made thin, and the probe - sensitive. The dimensions of the chamber and throttle tube are small otherwise the membrane could suffer rupture during pressure surges.

The probe represents a rigid and sufficiently durable construction. All basic components are made of stainless steel, the membrane of Permalloy. The feeler, glued to membrane with BF-2 glue, is made of Konstantan wire with a diameter of 0.03 mm and it has a spiral form, resistance of feeler 100-150 ohms. The qualities of the probe allow to use same not only in lab conditions, but also under natural conditions during stand and station testings of machines. These probes were used in testing natural GT-12-3 compressors.

In these investigations were fixed and measured the pulsating pressures on rotating compressor vanes (and as is known to us, for the first time). In working vanes with maximum thickness of 2 mm, were made chambers, in which were situated membranes with tenscometric probes (fig.2,b). The chambers were covered with lids having drainage openings with a diameter of 0.8 mm. The arrengement of feelers on the working vanes is shown in fig.2,a. Feeding the signal into amplifying and recording apparatus is realized through a mercury current stripper.

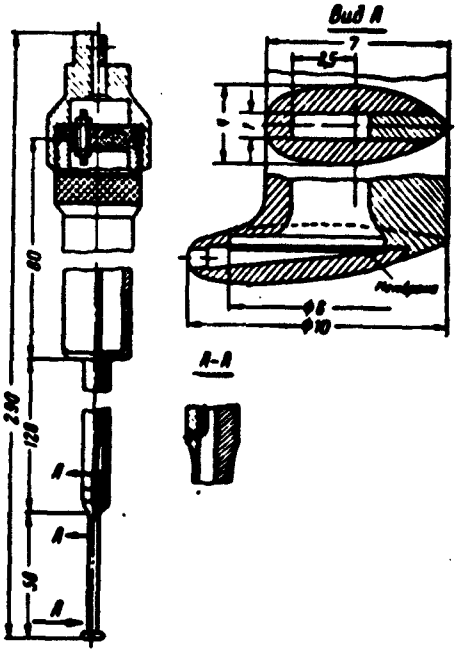

Fig.1. Tenscometric probe for full pressure with balanced membrane

To measure stresses in vanes of a working wheel and guide apparatus tenscometric feelers were glued to the vanes. The lead out of the signal from rotating vanes is also realized through a mercury current stripper.

The described apparatus gave the possibility of studying unstable aerodynamic phenomena and dynamic stresses in the vanes caused by them.

We shall discuss the experimental results.

In fig.3 is plotted the ordinary characteristic (curve 1) of the compressor in

coordinates

$$\varphi = \frac{c_a}{u} \text{ и } \psi = \frac{\Delta p}{\rho u^2}. \quad (2)$$

where c_a - axial velocity at input into the first guide apparatus; u- circuferential velocity on outer diameter; Δp - total increased pressure in compressor ; ρ density of air at input.

The characteristic curve has three branches. Normal operations branch situated in zone $\varphi > 0.4$. When φ drops to 0.4 and below in the compressor stages appears a rotating separation and the pressure coefficient ψ drops (second branch). The third branch ψ corresponds to a rise in the φ coefficient from 0 to $\varphi = 0.45$. It is evident from fig.3., that a hysteresis phenomenon originates: departure of grids from the separation takes place at smaller angles of attack, than the input into the stripping condition of flow.

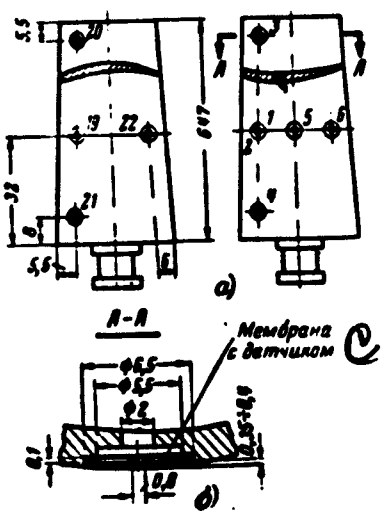

Fig.2. a-arrangement of tensometric feelers on working vanes of second stage of compressor; b- arrangement of membrane with feeler.c-membrane with feeler

Presence of rotating separation (break-away) is confirmed by direct measurements with the aid of tensometric probes. In fig.4 is given an oscillogram recording the total pressure behind the second working wheel with the aid of two low-inertia probes. Phase displacement of two processes indicates rotation of the separation, because the probes are situated in the plane of the wheel at a certain angle relative to each other. The rate of the rotating separation appears to be a stable value and is practically independent from φ. This is confirmed by measurement results, shown in fig.5, where along the axis of the ordinates is plotted the rate of rotation of the break-away zone relative to the stationary observer in fractions of circumferential speed of the vanes.

In some working conditions are observed two stably rotating zones, and in this case their rate of displacement relative to the stationary observer is reduced some what.

Measurements showed, that separation originated immediately over the entire height of the vanes and embraced all aerodynamic grids. The relative area of the separation zone e is in approximate linear dependence upon φ (fig.6), which is observed in all experiments in rotating separation.

We want to point out that rotating separation originated immediately during flow separation in the working grid, i.e. the appearance of stable stationary (in relative movement) simultaneous separation on all vanes , was not observed. These results were obtained during the processing of films, on which were recorde the pressure pulsations on the working vanes. At normal nonseparating working conditions the pressure pulsation on the vane is very low in comparison with pressure pulsation, appearing during separation. We will analyze the oscillograms pertaining to these investigations.

Oscillogram a of that series (fig.7)* pertains to the zone of normal compressor operation (φ = 0.398; ψ = 0.485), and consequently the indications of the pressure probe recorded in form of weak pulsation, indicating, that the flow around the grid is stable. Oscillograms b and c pertain to the second work zone (φ = 0.372; ψ = 0.456 and φ = 0.282; ψ = 0.41). The curve of pressure feeler indications appears to be periodic and consists of sections of straight lines, alternating with zones of strong pressure pulsations. It is apparent, that wherever the feeler registers constant pressure, the working grid is in nonseparable conditio , and wherever pulsation does appear, it goes into separation.

Examining the following oscillograms all the way up to oscillogram d, corresponding to total discontinuation of consumption (φ = 0), it can be ascertained, that the zone of separation encompasses the entireworking grid; the feeler records large

* In fig.7 and 8: upper curves-recording of dynamic stresses; central curves - recording of pressure pulsation on the profile, lower curves - recordings of timer (500 c).

graphic not reproducible

pressure pulsations.

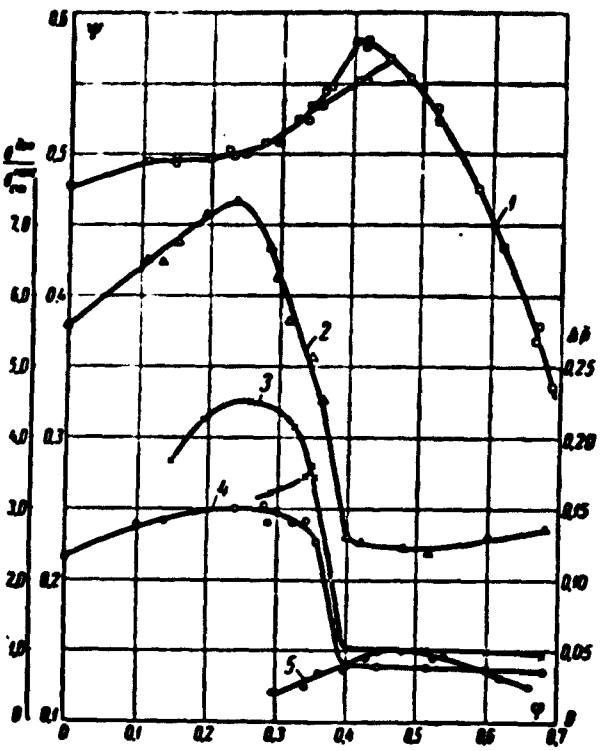

Fig.3. Summary characteristics
1-characteristic of compressor φ-ψ; 2-dimensionless dynamic stresses in guide vanes $\sigma_{dyn}/\sigma^{max}_{st}$ = f7(φ); 3-dimensionless curve of ststic pressure pulsation on rotating vanes; 4-dimensionless dynamic stresses in working vanes $\sigma_{dyn}/\sigma^{max}_{st} = f(\varphi)$; 5-dimensionless static stresses in working vanes $\sigma_{st}\ \sigma^{max}_{st} = f(\varphi)$

Fig.4. Total pressure on second working wheel.

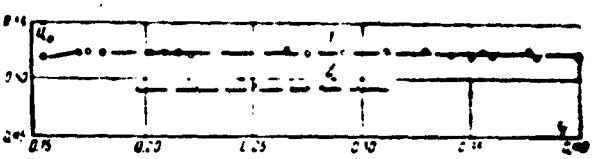

Fig.5. Dependence of rate of rotation of separations of the u_{sep} zone upon the consumption coefficient φ
1-one separation zone; 2-two separation zones.

Prior to the experiment all tensometric pressure sensing elements were calibrated by static pressure. In the assembled circuit of tensometric amplifier bridge parallel to the sensing element is connected a group of resistors, on which a resistance 9-10 kohms was selected. By changing this shunting resistance the bridge is debalanced equal to the unbalance from the probe at a definite pressure drop on the membrane. In this way it is possible to accurately establish the drop on the membrane of the sensing element of probe. This relationship is preserved for any sensitivity and for any registering apparatus. During the experimentation is possible by changing the shunt resistance into a calibration value to obtain a jump in recording probe indications which allows to decode the pressure pulsation amplitude recording in the vane apparatus.

As result of analyzing these observations was obtained a dependence of pressure

pulsation level at various working conditions of the compressor.

graphic not reproducible

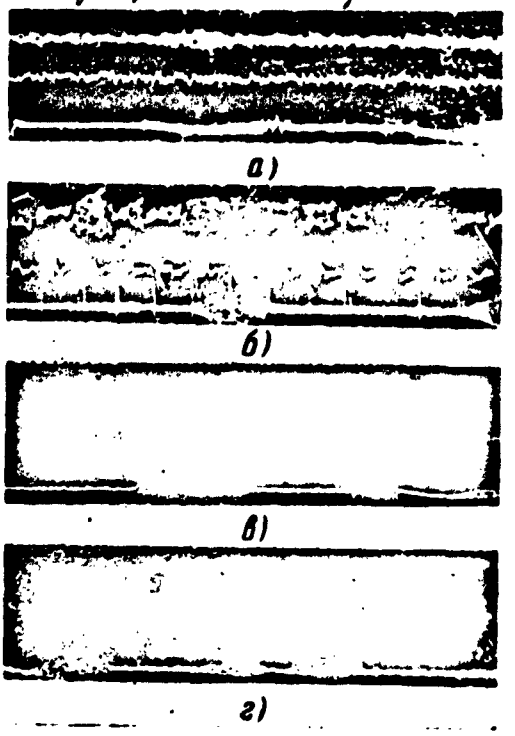

Fig.7. Oscillograms of dynamic stresses in working vanes and pressure pulsations in them. a-normal work zone; $\varphi = 0.398$; $\psi = 0.485$; b and c- separation work zone: $\varphi = 0.372$; $\psi = 0.456$; $\varphi = 0.282$; $\psi = 0.41$; d-work zone at zero consumption; $\varphi = 0$.

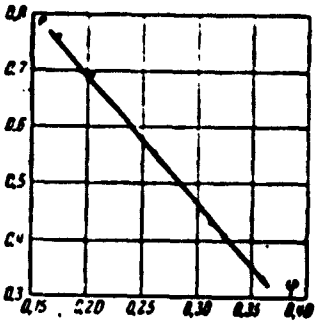

Fig.6. Dependence of relative area of separation zone e upon coefficient of consumption φ

In fig.3 is given the obtained in such way curve of static pressure pulsation level on the profile of the vane. Along the axis of the ordinates is plotted the dimensionless value $\overline{\Delta p} = 2\Delta p/\rho w_1^2$, i.e. pressure pulsation Δp taken in fractions of kinetic energy of flow in relative movement when entering the working grid at maximum pressure.

Upon the appearance of a rotating separation the level of pulsations rises by leaps and bounds. The pressure surges $\overline{\Delta p}$ at rotating separation constitute approximately 22% of the kinetic input energy, which causes a sharp rise in dynamic stresses in the vanes. Pressure pulsations taken from oscillograms (fig.7 and 8).

During the experiments were measured the dynamic stresses in working and guide vanes, and the corresponding static pressures as well.

In fig.3 are shown curves 2 and 4 of maximum in given case dynamic stresses in working and guide vanes, referred to corresponding static stresses at maximum pressure of the stage. Upon the appearance of rotating separation the dynamic stresses in the vanes, oscillating with natural frequency, constitute approximately 30-% of

corresponding maximum static pressures.

Simultaneous recording of dynamic stresses and pressure pulsations on the working vanes (fig.7) allows to study the interesting phenomenon.

As is evident from the oscillograms in a majority of compressor working conditions the periodicity of stress rise in the vanes is equal to the period of rotating separation; but in some working conditions there is no such conformity and stresses of flutter nature are predominant. This pertains especially to guide vanes (fig.8) which is apparent, and explained by their performance in separation media. The rotating zone has in its beginning during the movement relative to a stationary observer a maximum pressure pulsation amplitude; at the end of passing the zone of separation the amplitude of pressure pulsations decreases. Since rotor vanes catch up with the zone of rotating separation (relative to stationary observer), which revolves at a rate, lesser, than the rotor, pressure pulsation are increasing, which is evident on the oscillograms fig.7. In the guide vanes - phenomenon is in reverse: there is a decrease in pulsation in rato to passing the separation zone. This is also evident from the oscillogram fig.8. In working vanes is observed first a flash-up of stresses at the input into the separation zone, after which the stresses drop, in spite of the fact, that the pressure pulsation amplitude at the output from the separation zone rises in comparison with the entry into it. This phenomenon is explained by the fact, that the working vane having fallen into the zone of rotating separation

receives an excitation pulse. During this very same period, consisting of the rotating zone and normal work fragment, the vane calms down (stress amplitude decreases, fig.8,b.

The period of stress rising and falling is equal to the period of rotating separation. Particularly clearly visible are the stress drop and rise periods where rotating separation has the least relative length, in the point, where the zones of rotating separation have a diffused nature, the oscillograms of dynamic stresses have clear period either.

About static stresses in working vanes and the nature of their change opinions can be made from oscillograms and plotted resultant curve 5 in fig.3.

The experimental curve of static stresses has a maximum, corresponding to maximum pressure of the compressor, and it drops with the decrease in delivery (consumption). The static stresses curve does not pass through the beginning of coordinates, because the working vanes have a certain heaping in the plane of rotation and that is why we have a constant component of static stresses.

Static stresses were taken down with repeated checking of the balancing of the tensometric apparatus when passing characteristic work conditions. The basic characteristics were repeated and connected with each other several times, so as to gain the possibility of ascertaining that the balancing and indication correctness of the recording instrument are preserved. The magnitude of the stresses was evaluated by the calibration pulse of the measuring tensometric apparatus.

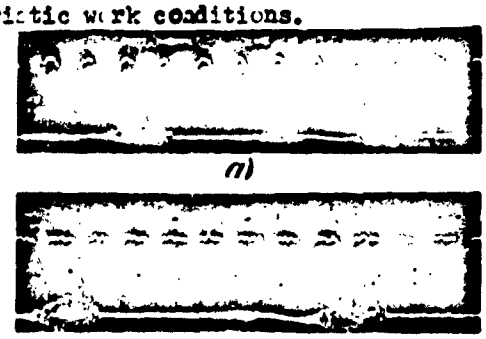

Fig.8. Oscillograms of dynamic stresses in guide vanes and pressure pulsations on them.

Literature

1. G.S.Samoylovich; G.A.Khanin. Report in LPI collection "Investigation of Elements of Steam and Gas Turbines and Axial Compressors" No.6, 1960

2. M.Ye.Deych, G.S.Samoylovich; Aerodynamic Bases of Axial Turbines, Mashgiz, 1959

3. G.S.Samoylovich; Ye.V.Mayorskiy; I.Neruda; Ye.V.Stekol'shchikov "TEPLOENERGETIKA" No1. 1959

DISTRIBUTION LIST

DEPARTMENT OF DEFENSE	Nr. Copies
HEADQUARTERS USAF	
AFCIN-3D2	1
ARL (ARB)	1
OTHER AGENCIES	
CIA	1
NSA	6
DIA	9
AID	2
OTS	2
AEC	2
PWS	1
NASA	1
ARMY	3
NAVY	3
RAND	1
NAFEC	1

MAJOR AIR COMMANDS	Nr. Copies
AFSC	
SCFDD	1
ASTIA	25
TDBTL	5
TDBDP	5
SSD (SSF)	2
BSD (BSF)	1
AFFTC (FTY)	1
AFSWC (SWF)	1
ASD (ASYIM)	1
ESD (ESY)	1
TDEPA	1